plant biology

Plant Biology ISSN 1435-8603

RESEARCH ARTICLE

Loss of function mutations at the tomato *SSI2* locus impair plant growth and development by altering the fatty acid desaturation pathway

A. S. Quevedo-Colmena[1], A. Ortiz-Atienza[1], M. Jáquez-Gutiérrez[2], M. Quinet[3], A. Atarés[2], F. J. Yuste-Lisbona[1], V. Moreno[2], T. Angosto[1] & R. Lozano[1]

1 Centro de Investigación en Biotecnología Agroalimentaria (CIAIMBITAL), Universidad de Almería, Almería, Spain
2 Instituto de Biología Molecular y Celular de Plantas (UPV-CSIC), Universidad Politécnica de Valencia, Valencia, Spain
3 Université catholique de Louvain, Ottignies-Louvain-la-Neuve, Belgium

Keywords
CRISPR/Cas9; jasmonic acid; plant growth; salicylic acid; *Solanum lycopersicum*; stearoyl-ACP desaturases.

Correspondence
F. J. Yuste-Lisbona and T. Angosto, Departamento de Biología y Geología (Genética), Edificio CITE II-B, Universidad de Almería, Carretera de Sacramento s/n, Almería 04120, Spain.
E-mail: fyuste@ual.es; tangosto@ual.es

Editor
T. Bisseling

Received: 28 May 2023;
Accepted: 24 October 2023

doi:10.1111/plb.13591

ABSTRACT

- The stearoyl-ACP desaturase (SACPD) is a key enzyme in the regulation of saturated to unsaturated fatty acid ratio, playing a crucial role in regulating membrane stability and fluidity, as well as photosynthesis efficiency, which makes it an important research focus in crop species.
- This study reports the characterization and molecular cloning of *pale dwarf* (*pad*), a new tomato (*Solanum lycopersicum* L.) T-DNA recessive mutant, which exhibits a dwarf and chlorotic phenotype. Functional studies of the T-DNA tagged gene were conducted, including phylogenetic analysis, expression and metabolomic analyses, and generation of CRISPR/Cas9 knockout lines.
- The cloning of T-DNA flanking genomic sequences and a co-segregation analysis found the *pad* phenotype was caused by a T-DNA insertion disrupting the tomato homologue of the *Arabidopsis SUPPRESSOR OF SALICYLIC ACID INSENSITIVITY 2* (*SlSSI2*), encoding a plastid localized isoform of SACPD. The phenotype of CRISPR/Cas9 *SlSSI2* knockout lines confirmed that the morphological abnormalities in *pad* plants were due to *SlSSI2* loss of function. Functional, metabolomic and expression analyses proved that *SlSSI2* disruption causes deficiencies in 18:1 fatty acid desaturation and leads to diminished jasmonic acid (JA) content and increased salicylic acid (SA) levels.
- Overall, these results proved that SSI2 plays a crucial role in the regulation of polyunsaturated fatty acid profiles in tomato, and revealed that *SlSSI2* loss of function results in an inhibited JA-responsive signalling pathway and a constitutively activated SA-mediated defence signalling response. This study lays the foundation for further research on tomato SACPDs and their role in plant performance and fitness.

INTRODUCTION

Lipids are the primary components of biomembranes and essential molecules for life, as they are required for energy production, signalling pathways and membrane structure (Van Meer *et al.* 2008). The lipid composition of plant membranes is mainly distinguishable from that of animals and fungi for its high content in polyunsaturated fatty acids (Webb & Green 1991). In the plant kingdom, fatty acids are essentially *de novo* synthesized in the plastids (Ohlrogge & Browse 1995), giving rise to the formation of palmitic acid (16:0) and stearic acid (18:0) conjugated to acyl-carrier protein (ACP) (Somerville *et al.* 2000). The stearoyl-ACP desaturase (SACPD) is a key enzyme catalysing 18:0-ACP conversion to oleic acid (18:1)-ACP in the chloroplast stroma (Kachroo *et al.* 2007). The 16:0-ACP and 18:1-ACP serve as principal substrate for the glycerol-3-phosphate acyltransferase, leading to the formation of phosphatidic acid and other fatty acids that are subsequently incorporated into membrane glycerolipids, such as mono- and digalactosyl diacylglycerol, which account for 70–80% of the total lipids in chloroplast membranes and play a vital role in regulating membrane stability and fluidity, as well as photosynthesis efficiency (Kobayashi *et al.* 2016; He *et al.* 2020).

The SACPD function is crucial in plants as its activity regulates the ratios of saturated to unsaturated fatty acids. SACPD catalyses 18:1 production, which can then be desaturated into polyunsaturated fatty acid derivatives, such as linolenic acid (18:2) and alpha-linolenic acid (18:3) (He *et al.* 2020). Polyunsaturated fatty acid levels, in addition to affecting membrane lipid fluidity, also regulate the formation of fatty acid derived cyclopentanones, including the phytohormone jasmonic acid (JA) and its volatile methyl ester, MeJA, which are synthesized by the octadecanoid pathway using mainly 18:3 as precursor (Wasternack & Song 2017). Cross-communication between JA-mediated signalling and salicylic acid (SA)-associated response has been reported to be mediated by the basic-helix–loop–helix transcription factor MYC2, a master regulator of JA signalling in the model species *Arabidopsis thaliana* (Kazan & Manners 2013). As a result, disturbances to polyunsaturated fatty acid levels can lead to alterations in JA- and SA-mediated responses, which drive numerous signalling pathways involved in a range of developmental processes and in reactions to

abiotic and biotic stresses (Wasternack & Song 2017; Lefevere *et al.* 2020).

Even though up to seven isoforms of genes encoding SACPD have been identified in the *Arabidopsis* genome (Kachroo *et al.* 2007), it has been shown that loss of function of the *SUPPRESSOR OF SALICYLIC ACID INSENSITIVITY 2* (*SSI2*) gene is sufficient to give rise to severe growth and developmental defects (Kachroo *et al.* 2001; Shah *et al.* 2001). Mutant plants in *SSI2* are pale and reduced in size, spontaneously develop hypersensitive response-like lesions on their leaves and have an increased level of 18:0 caused by their ineffectiveness in catalysing the 18:1 formation in chloroplasts (Kachroo *et al.* 2001). These decreased levels of 18:1 simultaneously result in the activation of a SA-mediated response and the suppression of JA-inducible signalling, leading to the constitutive activation of pathogenesis-related genes, the induction of hypersensitive response and an enhancement of broad-spectrum resistance to oomycete and bacterial pathogens (Shah *et al.* 2001; Kachroo *et al.* 2003, 2004; Chandra-Shekara *et al.* 2007; Venugopal *et al.* 2009; Xia *et al.* 2009; Gao *et al.* 2011). The occurrence of growth and developmental alterations and induction of defence responses seems to be conserved among different plant species upon loss of SACPD activity. Thus, reduction of 18:1 levels through virus-induced gene silencing of *GmSACPDs* and *GhSACPDs* in soybean (*Glycine max*) and cotton (*Gossypium hirsutum*), respectively, apart from resulting in necrotic lesions in leaves and a decrease of plant height, triggers a constitutive activation of defence signalling and greater resistance to several pathogens (Kachroo *et al.* 2008; Mo *et al.* 2021). Likewise, RNA interference mediated knockdown of the *SSI2* rice (*Oryza sativa*) homologue (*OsSSI2*) causes stunted plant growth, lesion formation in leaf blades and an increase in the resistance to fungal blast and bacterial leaf blight diseases (Jiang *et al.* 2009).

In this work, we report the molecular cloning and characterization of the tomato (*Solanum lycopersicum*) *pale dwarf* (*pad*) mutant, which was isolated from the screening of a T-DNA mutant collection. Seedlings of the *pad* mutant show severe growth and developmental defects including leaves with altered morphology, chlorosis and necrotic lesions. By determining the genomic regions flanking the transgene insertion site, we found that the T-DNA insertion in *pad* mutants disrupts the tomato homologue of the *Arabidopsis SSI2* gene (*PAD/SlSSI2*). Through functional, metabolomic and expression analyses, we prove that *PAD/SlSSI2* gene activity is crucial in regulating 18:1 levels, which in turn promotes repression of the JA-responsive signalling pathway, as well as the constitutive activation of SA-mediated defence signalling response.

MATERIAL AND METHODS

Plant material and growth conditions

The *pad* mutant was isolated from a T-DNA insertional collection, which was generated in the genetic background tomato cultivar Moneymaker through infection with *Agrobacterium tumefaciens* strain LBA4404 containing the pBI121 binary vector (Chen *et al.* 2003). The TG_1 line was self-pollinated to obtain the TG_2 progeny, which were grown in soil under greenhouse conditions using standard practices, with regular addition of fertilizers. As *pad* mutant homozygous plants did not survive long enough to achieve fruit set, *pad* lines were perpetuated by self-pollination of wild-type heterozygous plants. For *in vitro* assessment of *pad* mutant phenotype, plants were grown on Murashige and Skoog agar medium. *In vitro* co-segregation studies of the *pad* phenotype with kanamycin resistance were carried out by sowing seeds on Murashige and Skoog agar medium supplemented with kanamycin ($100\ mg{\cdot}l^{-1}$) and sucrose ($10\ g{\cdot}l^{-1}$).

Cloning of T-DNA flanking sites and PCR genotyping

Anchor-PCR was performed to clone the genomic sequences flanking the *pad* T-DNA insertion according to the procedure previously established by Pérez-Martín *et al.* (2017). The cloned sequences were compared with the SGN Database (http://solgenomics.net/) to assign the T-DNA insertion site on the tomato genome (ITAG4.0). Co-segregation of the T-DNA insertion site with the mutant phenotype was carried out in the TG_2 progeny using the SlSSI2_F and SlSSI2_R primers (to amplify the wild-type allele, without T-DNA insertion), and the specific T-DNA border primer RightBorder1 and the SlSSI2_R primer (to amplify the mutant allele, carrying the T-DNA insertion). Genotyping PCR was performed in a volume of 30 µl using 25 ng of total DNA, 50 ng of each primer, 0.25 mM dNTPs, 2.5 mM $MgCl_2$, and 1 U BIOTAQ™ DNA Polymerase (Bioline, London, UK) in 1× Taq buffer. The following thermal cycling conditions were used: 94 °C for 5 min, followed by 35 cycles at 94 °C for 30 s, 60 °C for 30 s, and 72 °C for 2 min, and a final extension of 5 min at 72 °C. PCR products were electrophoresed in 1% agarose gels in SB buffer (200 mM NaOH, 750 mM boric acid, pH 8.3) and visualized with GelRed Nucleic Acid Stain (Biotium, Fremont, CA, USA). Primers used for anchor-PCR and genotyping are provided in Table S1.

Generation of CRISPR/Cas9 lines

The CRISPR/Cas9 mutagenesis was performed according to the protocol described by Vazquez-Vilar *et al.* (2016). Breaking-Cas software (Oliveros *et al.* 2016) was used to design the single guide RNA (sgRNA) target sequence (GGGCC ATTTGGACAAGAGCT) within the coding region of the *SlSSI2* (Solyc06g053480) gene. The CRISPR/Cas9 construct contained the *Arabidopsis* U626 promoter to express the sgRNA constitutively, as well as the transcriptional unit for (human codon optimized) Cas9 plant expression driven by the 35S promoter and the kanamycin resistance gene as a selective marker. Genetic transformation experiments were carried out as described in Ellul *et al.* (2003) using *Ag. tumefaciens* strain LBA4404. The ploidy levels of TG_1 transgenic plants were assessed by flow cytometry following the protocol described by Atarés *et al.* (2011). Each TG_1 plant was genotyped with primers that cover the target recognition region of the sgRNA (Table S1). PCR products were purified and cloned into the pGEMT vector (Promega, Madison, WI, USA). A minimum of 10 clones per PCR product were sequenced to characterize the edited alleles carried by TG_1 plants.

Chlorophyll content and fatty acid profile quantification

Chlorophylls were extracted from 0.5 g fresh leaf tissue for each sample following the procedure previously described by Lichtenthaler & Wellburn (1983). Chlorophyll content, including *a*,

b, and total chlorophyll, were determined based on ultraviolet–visible spectroscopy and calculated as $\mu g \cdot g^{-1}$ fresh weight of leaf tissue according to the method described by Arnon (1949).

The extraction of total fatty acids was carried out as described by Dahmer *et al.* (1989). Briefly, 0.5 g lyophilized leaf tissue from each sample (at similar size and age) were placed in 2 ml 3% H_2SO_4 in methanol containing 0.001% butylated hydroxytoluene. After 30 min incubation at 80 °C, 1 ml hexane with 0.001% butylated hydroxytoluene was added. We used 1 µl samples of the hexane phase for gas chromatography on a Varian FAME 0.25 mm × 50 m column (Varian Inc., Palo Alto, CA, USA) and quantified with flame ionization detection. Fatty acid quantification was carried out using nonadecanoic acid methyl ester (19:0; Sigma-Aldrich, St. Louis, MO, USA) as internal standard and by conversion of relative peak areas into weight percentages. The identities of the peaks were determined by comparing their retention times with those of known fatty acid standards. Fatty acid content was expressed as $\mu g \cdot 100\ mg^{-1}$ dry weight of leaf tissue.

Evaluation of JA and SA levels

Acid hormone levels were quantified at the Plant Hormones Quantification platform (IBMCP, Valencia, Spain). The analysis was performed on 0.1 g leaf tissue, which was suspended in 80% methanol–1% acetic acid containing internal standards and mixed by shaking for 1 h at 4 °C. Deuterium-labelled SA and dhJA (OlChemim, Olomouc, Czech Republic) were used as internal standards for quantification of SA and JA, respectively. The extracts were kept a −20 °C overnight, then centrifuged and the supernatant dried in a vacuum evaporator. The dry residues were dissolved in 1% acetic acid and passed through a reverse phase column (Oasis HLB 30 mg; Waters, Milford, MA, USA), as described in Seo *et al.* (2011). The extracts were additionally passed through a cation exchange (Oasis MCX, Waters; and Strata X-C, Phenomenex, Torrance, CA, USA). To recover the acid fraction, the dried samples were eluted with 100% methanol–1% acetic acid. The final residues were dried and dissolved in 5% acetonitrile–1% acetic acid and the JA and SA hormones separated by Ultra High Performance Liquid Chromatography-Mass Spectrometry in a reverse Accucore C18 column (2.6 µm, 100 mm length; Thermo Fisher Scientific, Waltham, MA, USA) with an acetonitrile gradient containing 0.05% acetic acid.

The JA and SA hormones were analysed using a Thermo Scientific™ Q Exactive™ Hybrid Quadrupole-Orbitrap Mass Spectrometer (Thermo Fisher Scientific) by targeted Selected Ion Monitoring (tSIM; capillary temperature 300 °C, S-lens RF level 70, resolution 70,000) and electrospray ionization (spray voltage 3.0 kV, heater temperature 150 °C, sheath gas flow rate 40 $\mu l \cdot min^{-1}$, auxiliary gas flow rate 10 $\mu l \cdot min^{-1}$) in negative mode. The concentrations of JA and SA hormones in the extracts were determined using embedded calibration curves and the Xcalibur 4.0 and TraceFinder 4.1 SP1 programs (Thermo Fisher Scientific).

Quantitative real-time PCR analysis

Total RNA was isolated from leaves using TRIZOL (Invitrogen Life Technologies, San Diego, CA, USA) according to the manufacturer's instructions and treated with TURBO DNase (Ambion, Austin, TX, USA) to remove contaminating DNA. Reverse-transcription and quantitative Real-Time PCR (qRT-PCR) analyses were performed as described in Pérez-Martín *et al.* (2018). qRT-PCR amplifications were performed on a 7300 Real-Time PCR System (Applied Biosystems, Foster City, CA, USA) using three biological and two technical replicates for each genotype. The housekeeping gene *Ubiquitin3* (*Solyc01g056940*) was used as control. Quantification of relative gene expression was determined using the ΔΔCt calculation method (Winer *et al.* 1999). Specific primer pairs for each gene evaluated by qRT-PCR are listed in Table S2.

RESULTS

The *pad* plants exhibit stunted growth and a chlorotic phenotype

The *pad* mutant was isolated from the screening of a tomato T-DNA collection generated in the genetic background cultivar Moneymaker. The *pad* mutant was selected as it showed a dwarf and chlorotic phenotype in greenhouse conditions; thus, after 45 days of culture the mutant plants reached no more than 10 cm in height (Fig. 1a). In addition, chlorophyll content was significantly reduced in *pad* mutant leaves (Fig. 1b), supporting that the pale colour of *pad* was caused by a severe deficiency in the photosynthetic machinery. Under *in vitro* conditions, leaf chlorosis and a decline in plant growth were less apparent in *pad* plants (Fig. 1c–e), their cotyledons remained green, and chlorosis was mainly restricted to the leaves (Fig. 1d), although they maintained similar morphology and phyllotaxis to wild-type (WT) plants (Fig. 1g). In contrast, *pad* plants grown *in vivo* showed alterations to the leaf morphology with decreased development of secondary and tertiary leaflets, as well as displaying progressive chlorosis and the occurrence of necrotic lesions in apices of the older leaves (Fig. 1f). Together, this set of alterations leads to the death of *pad* mutant plants before reaching the reproductive stage.

As regards root development, primary root growth was not affected in *pad* mutants. However, the growth of lateral roots was lower in both embryo-derived roots (Fig. 1h) and adventitious root system (Fig. 1i), resulting in the formation of a less branched root system than that in WT plants. To ascertain whether the vegetative *pad* phenotype is determined by root alterations, reciprocal grafting experiments were performed between WT and *pad* plants. Grafted plants developed chlorotic and smaller leaves when *pad* was used as scion, independently of the rootstock background, while a WT phenotype was observed in leaves when WT scion was grafted on either WT or *pad* rootstock (Fig. 1j). Therefore, it is possible to conclude that the chlorosis and the severe reduction in vegetative growth found in *pad* mutant plants was not due to alterations in the root system architecture.

The *pad* mutant line bears a T-DNA insertion located in the tomato homologue of *SSI2*

Genetic analyses were performed in a TG_2 progeny of 177 seedling plants, which were likewise screened *in vitro* for kanamycin resistance. Results suggested that the *pad* phenotype is caused by a single-gene recessive mutation, although the data obtained deviated from the expected segregation for a single T-DNA

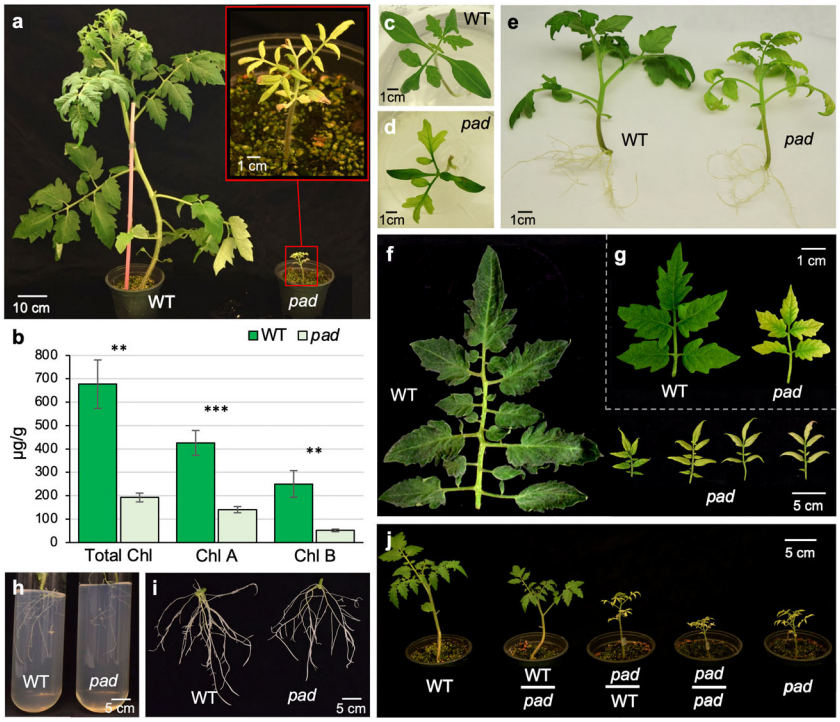

Fig. 1. Phenotypic characterization of *pad* insertional mutant. (a) Wild-type (WT) and *pad* plants grown in greenhouse conditions for 45 days. (b) Chlorophyll (Chl) content in WT and *pad* plants. Data are mean of $\mu g \cdot g^{-1}$ fresh weight of leaf tissue ± SD (n = 3). Significant differences detected using Student's *t*-test are represented by asterisks: $^{**}P < 0.001$; $^{***}P < 0.0001$. (c–e) WT and *pad* plants grown under *in vitro* conditions for 10 (c, d) and 21 (e) days. (f, g) Leaves of WT and *pad* plants after 30 days growing under greenhouse (f) and *in vitro* (g) conditions. (h, i) Embryo-derived (h) and adventitious (i) root systems of WT and *pad* plants grown under *in vitro* conditions for 24 days. (j) Grafted plants between WT and *pad* grown in greenhouse conditions for 30 days.

insertion (1:2:1 ratio; 61 WT and kanamycin susceptible:89 WT and kanamycin resistant:27 mutant and kanamycin resistant; $\chi^2 = 1.18$ E-05; $P = 0.003$). This segregation distortion could be due to the partial penetrance of the embryonic lethality of homozygous plants. Nevertheless, it is noteworthy that a complete co-segregation was found between *pad* mutant and kanamycin-resistance phenotypes, as the 27 *pad* plants identified were also resistant to kanamycin, suggesting that the T-DNA insertion was responsible for the *pad* mutant phenotype.

To identify the gene tagged in the *pad* mutant, genomic regions flanking T-DNA insertion were cloned by anchor-PCR and their sequences were compared both to those of WT plants and the tomato reference genome (Tomato Genome Consortium 2012). Results revealed that the T-DNA insertion was located on chromosome 6 of the tomato genome, in the second intron of the *Solyc06g053480* gene (Fig. 2a), which encodes the tomato homologue of the *Arabidopsis* stearoyl-ACP-desaturase SSI2 (SlSSI2, Figure S1). Further sequence characterization also showed that the insertion event produced a 168 bp deletion in genomic DNA close to the T-DNA left border (Fig. 2a). In addition, a PCR co-segregation analysis was performed in the TG_2 progeny using allele-specific primers designed from both the T-DNA and the genomic flanking sequences tagged in the *pad* mutant. Co-segregation results revealed that all the plants carrying the T-DNA insertion in the homozygous state exhibited a *pad* mutant phenotype. In contrast, kanamycin susceptible WT plants were azygous for the T-DNA insertion, whereas kanamycin resistant WT plants were heterozygous (Fig. 2b). Together, these findings support the initial hypothesis of the partial penetrance of the embryonic lethality in plants homozygous for the T-DNA insertion, as well as indicating that the *pad* mutant phenotype was likely caused by a single copy T-DNA insertion that affects the *SlSSI2* gene.

The qRT-PCR experiments were carried out to monitor the *SlSSI2* gene transcriptional profile throughout development. *SlSSI2* exhibited ubiquitous expression, and its transcripts were detected in both vegetative and reproductive organs. The highest *SlSSI2* transcript accumulation was detected in fruits at red stage, leaves and flowers at anthesis day, whereas the lowest *SlSSI2* expression levels were found in roots (Fig. 2c). As *pad* plants did not reach the reproductive stage, the effects of T-DNA integration on *SlSSI2* gene expression were determined in leaf tissues, which clearly showed that the *SlSSI2* gene was drastically down-regulated in *pad* mutant leaves as no transcripts were detected when compared with WT values (Fig. 2d).

The *pad* mutation alters fatty acid composition

Considering that the loss of function of the *Arabidopsis SSI2* gene results in reduction of polyunsaturated fatty acid levels (Kachroo *et al.* 2001), and the T-DNA integration in *pad* mutants disrupts *SlSSI2* gene expression, the fatty acid composition of WT and *pad* leaves was analysed. Compared to WT plants, *pad* leaves had significantly higher levels of 18:0 but lower content of 18:1 fatty acid (Table 1). Thus, the levels of 18:0 fatty acid were increased six-fold in *pad* leaves, whereas 18:1 levels were 2.9-fold lower than the WT, which supports that the *pad* mutation affects *SlSSI2* gene activity, causing deficiencies in 18:0 fatty acid desaturation. Furthermore, accumulations of 16:3, 18:2 and 18:3 fatty acids significantly decreased

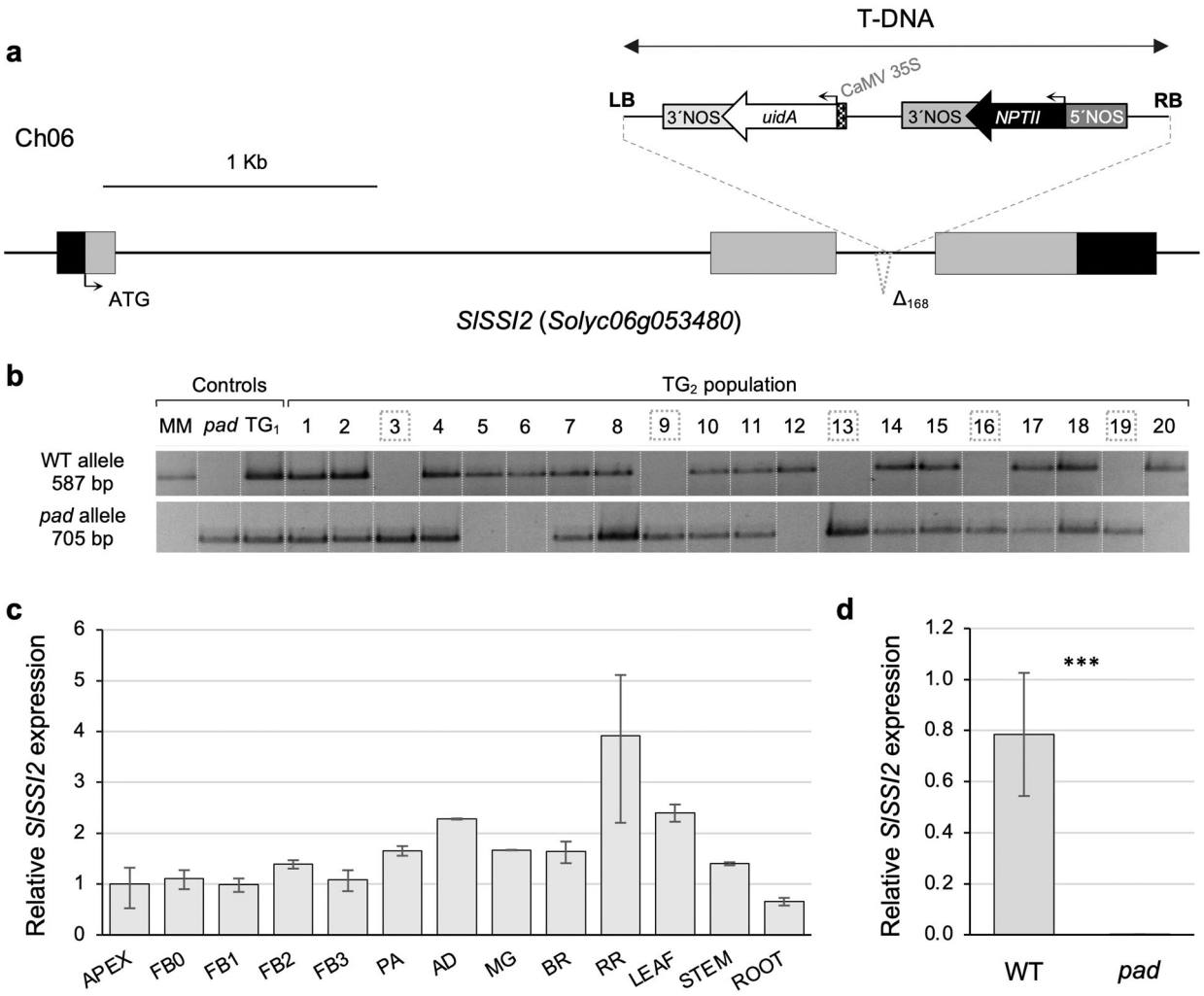

Fig. 2. Molecular characterization of *pad* insertional mutant. (a) Structure and position of the T-DNA insertion disrupting the *SlSSI2* gene. The T-DNA integration event caused a 168-bp deletion (Δ_{168}) in the *pad* line. Black boxes, grey boxes and lines between boxes represent 5′- and 3′-untranslated regions (UTRs), exons, and introns, respectively. ATG, transcription start site. (b) Co-segregation analysis of the T-DNA insertion and the *pad* phenotype in 20 plants of the TG_2 population. TG_2 plants heterozygous (1, 2, 4, 7, 8, 10, 11, 14, 15, 17 and 18) and homozygous for the wild-type (WT) allele (5, 6, 12 and 20) exhibited WT phenotype, whereas TG_2 plants homozygous for the mutant allele (3, 9, 13, 16 and 19) showed *pad* phenotype. Dashed rectangles indicate TG_2 plants presenting *pad* mutant phenotype. (c) Relative expression of the *SlSSI2* gene in different developmental tissues and stages of WT plants. FB0, floral bud of 0 to 2.9 mm in length; FB1, floral bud of 3.0 to 5.9 mm in length; FB2, floral bud of 6.0 to 8.9 mm in length; FB3, floral bud of 9.0 to 12.0 mm in length; PA, flower at preanthesis stage; AD, flower at anthesis stage; MG, mature green fruit; BR, breaker fruit; RR, red ripe fruit. (d) Relative expression of the *SlSSI2* gene in WT and *pad* mutant genotypes. Significant differences detected using Student's *t*-test are represented by asterisks: ***$P < 0.0001$.

in *pad* leaves. Regarding 16:0 and 16:1 fatty acids, their levels were similar to those of WT plants (Table 1).

The *SlSSI2* CRISPR/Cas9 knockout lines resemble the *pad* phenotype

To establish a direct causal relationship between the T-DNA integration in the *SlSSI2* gene and the observed *pad* mutant phenotype, knockout mutations of this gene were engineered using the CRISPR/Cas9 system with a sgRNA targeting its second exon (Fig. 3a). Molecular characterization of five independent TG_1 diploid lines (CR-*Slssi2*) revealed that three of them (CR-*Slssi2*-2, CR-*Slssi2*-3 and CR-*Slssi2*-4) bore mutant alleles edited in the region targeted by the sgRNA in homozygous state. The CR-*Slssi2*-2 and CR-*Slssi2*-3 plants carried the same AG deletion, while the CR-*Slssi2*-4 plant harboured a single A deletion (Fig. 3a). The remaining two lines, CR-*Slssi2*-1 and CR-*Slssi2*-5, were biallelic for edited mutant alleles. The CR-*Slssi2*-1 plant harboured single G and 241 bp deletions, whereas the CR-*Slssi2*-5 plant carried AAGA and ATTTGGACAAGA deletions (Fig. 3a). In summary, the molecular characterization of the five TG_1 CR-*Slssi2* lines led to the identification of a total of five different CRISPR/Cas9 alleles (Fig. 3a, Figure S2) whose transcripts contained open-reading frames predicted to be translated into proteins containing a truncated fatty acid desaturase domain (Figure S3). Hence, CRISPR/Cas9 editing would have given rise to knockout alleles that result in non-functional proteins. In agreement with this predicted function, all CR-*Slssi2* plants displayed leaf chlorosis and a decline in growth almost equal to that observed in *pad*

Table 1. Fatty acid composition of total leaf lipids from wild-type and *pad* mutant plants.

fatty acid	wild type	*pad*	
16:0	1338.37 ± 203.83	1440.82 ± 38.55	ns
16:1	19.99 ± 1.76	26.87 ± 2.76	ns
16:3	569.87 ± 104.44	132.23 ± 6.02	***
18:0	265.24 ± 38.51	1615.26 ± 73.08	***
18:1	191.82 ± 28.38	66.05 ± 4.16	***
18:2	1728.05 ± 220.37	1031.13 ± 87.14	**
18:3	2762.07 ± 441.23	1826.66 ± 87.48	***

Data are presented as mean of μg·100 mg^{-1} dry weight of leaf tissue ± SD (n = 3). Measurements were made on plants grown at 22 °C for 4 weeks. Significant differences detected using Student's *t*-test are represented by asterisks: *$P < 0.01$; **$P < 0.001$; ***$P < 0.0001$; ns, no statistically significant differences.

mutant plants (Fig. 3b, c). Furthermore, leaves of these CR-*Slssi2* plants also contained an altered fatty acid composition, having considerably higher levels of 18:0 fatty acids compared to the WT, as well as decreased content of polyunsaturated fatty acids such as 18:1 and 16:3 (Fig. 3d, Table S3). Therefore, these results confirmed that the T-DNA mutation affecting the *SlSSI2* gene was responsible for the stunted and chlorotic phenotype observed in the *pad* mutant, as well as the loss of function of the *SlSSI2* gene (hereafter referred to as *PAD/SlSSI2*) prevents conversion of 18:0 to 18:1, which leads to accumulation of 18:0 fatty acids.

The *pad* mutation reduces JA content and disrupts the JA-mediated signalling pathway

As JA biosynthesis uses mainly 18:3 fatty acids as precursor (Wasternack & Song 2017), and *pad* mutants had 1.5-fold lower 18:3 levels relative to WT plants, JA content was examined to assess to what extent its biosynthesis is altered by the loss of function of *PAD/SlSSI2*. A significant reduction of JA was found in *pad* plants compared to the WT (Fig. 4a), which probably resulted from a deficiency of the substrate 18:3 fatty acid for JA biosynthesis. Indeed, the mean value of JA content in WT leaves was 75.62 ± 29.79 ng·g^{-1} fresh weight (FW), while in *pad* leaves it was less than half (31.93 ± 2.78 ng·g^{-1} FW). The expression of JA pathway related genes was also evaluated by qRT-PCR. No significant differences were found between WT and *pad* plants in the expression of *LIPOXYGENASE D* (*SlLOXD*) (Fig. 4b), encoding a tomato chloroplast-localized lipoxygenase that catalyses the hydroperoxidation of 18:3 fatty acid, a key step in JA biosynthesis (Yan *et al.* 2013). In contrast, expression of the tomato *JASMONATE RESISTANT 1* (*SlJAR1*), involved in production of the bioactive JA jasmonoyl-L-isoleucine (Suza *et al.* 2010), was significantly upregulated in *pad* mutants (Fig. 4c). As regards genes related to the JA signalling pathway, its master regulator *SlMYC2* (Liu *et al.* 2019) was also significantly upregulated in *pad* plants (Fig. 4d), as well as expression of the tomato *MEDIATOR 25* (*SlMED25*) (Fig. 4e), which forms a transcriptional activation complex with SlMYC2 to activate the expression of JA-responsive genes (Liu *et al.* 2019). The expression levels of the

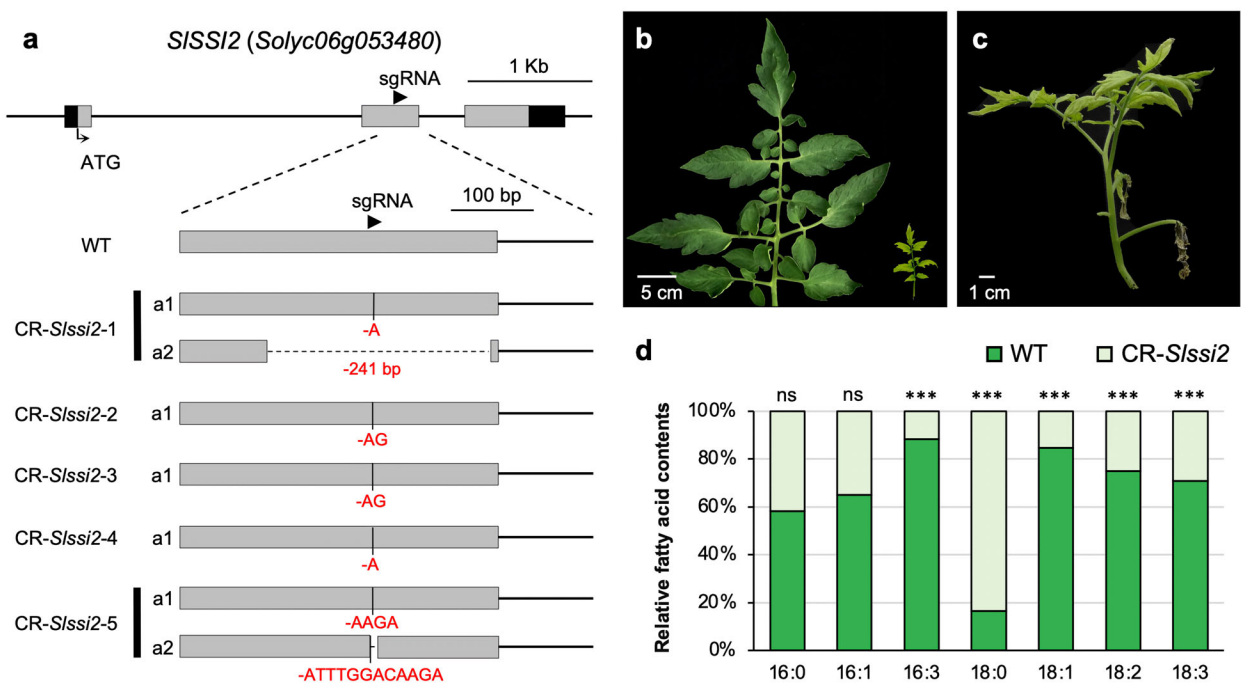

Fig. 3. Characterization of CRISPR/Cas9-*Slssi2* (CR-*Slssi2*) lines. (a) Schematic illustration of the *SlSSI2* gene structure, the single guide RNA (sgRNA) targeting the *SlSSI2* exon 2 (black arrow) and CR-*Slssi2* edited alleles identified in five independent TG_1 CR-*Slssi2* lines. Black boxes, grey boxes and lines between boxes represent 5′- and 3′-untranslated regions (UTRs), exons, and introns, respectively. ATG, transcription start site. Deletions are indicated by a minus symbol followed by the nucleotides lost by the mutant allele. (b) Representative leaf phenotype from CR-*Slssi2* lines compared with wild-type (WT). (c) Representative phenotype of a CR-*Slssi2* plant. (d) Relative fatty acid content of total leaf lipids from WT and CR-*Slssi2* plants. Measurements were made in plants grown at 22 °C for 4 weeks. Significant differences detected using Student's *t*-test are represented by asterisks: **$P < 0.001$; ***$P < 0.0001$; ns, no statistically significant differences.

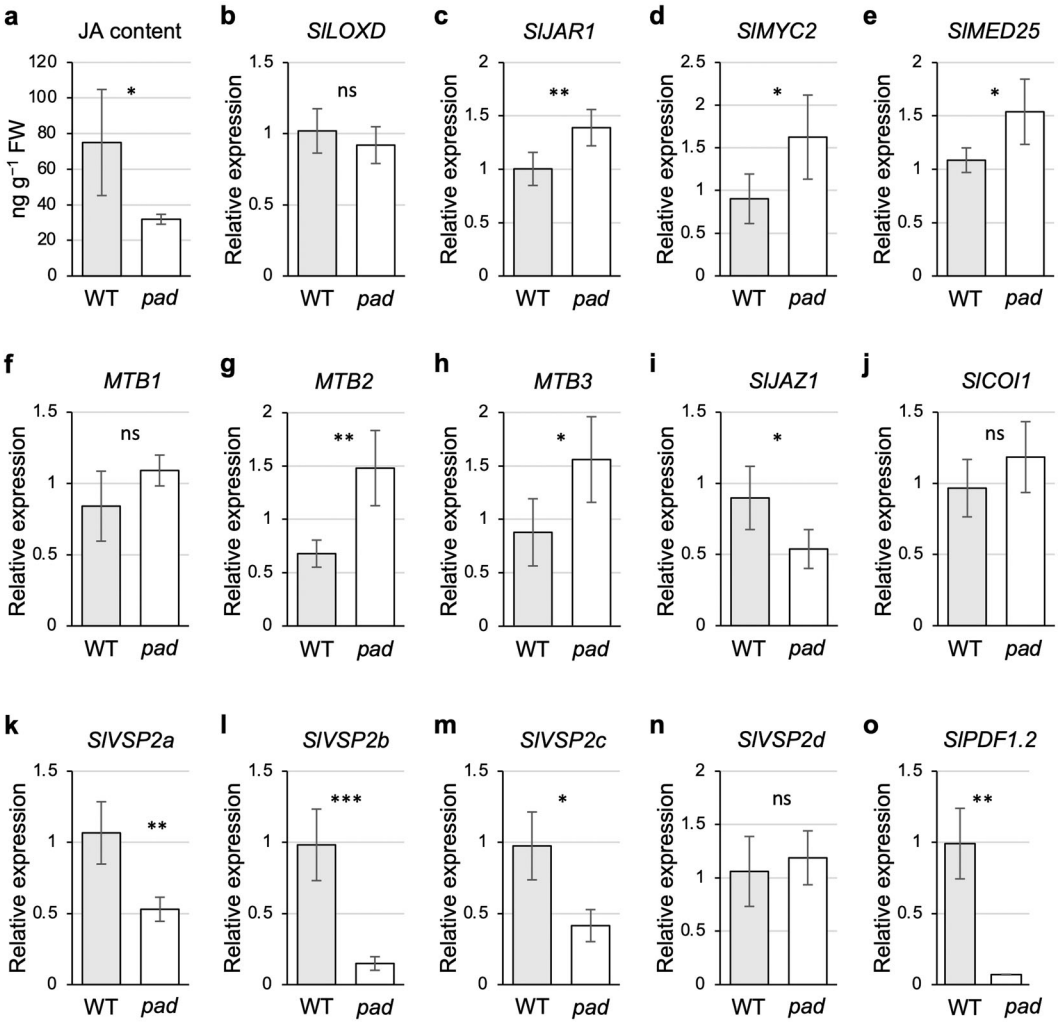

Fig. 4. Jasmonic acid (JA) content and relative expression levels of JA-related genes in wild-type (WT) and *pad* mutant plants. (a) Quantification of JA in leaves of WT and *pad* plants. (b–o) Relative expression by qRT-PCR of JA biosynthetic genes *SlLOXD* (b) and *SlJAR1*(c), and JA signalling pathway genes *SlMYC2* (d), *SlMED25* (e), *MTB1* (f), *MTB2* (g), *MTB3* (h), *SlJAZ1* (i), *SlCOI1* (j), *SlVSP2a* (k), *SlVSP2b* (l), *SlVSP2c* (m), *SlVSP2d* (n) and *SlPDF1.2* (o) in leaf tissues of WT and *pad* plants. Significant differences detected using Student's *t*-test are represented by asterisks: *$P < 0.01$; **$P < 0.001$; ***$P < 0.0001$; ns, no statistically significant differences.

JA-inducible *MYC2-TARGETED BHLH* (*MTB*) genes were also assessed. *MTBs* are homologues of the *Arabidopsis JASMONATE ASSOCIATED MYC2 LIKE* (*JAM*) genes and act to negatively regulate JA signalling (Liu *et al.* 2019). Thus, *MTB2* and *MTB3* genes were found to be significantly upregulated in *pad* plants, unlike *MTB1* gene expression that showed no significant differences (Fig. 4f–h). Furthermore, transcript levels of the homologue of the *Arabidopsis JASMONATE-ZIM-DOMAIN PROTEIN 1* (*SlJAZ1*), a negative regulator within the JA signalling pathway (Major *et al.* 2017), were found to be significantly downregulated in *pad* plants (Fig. 4i), whereas no differences were observed in expression of the tomato *CORONATINE-INSENSITIVE1* (*SlCOI1*) gene (Fig. 4j), which encodes an F-box protein required for JA-signalled processes (Li *et al.* 2004). With respect to JA-responsive genes, the expression levels of three out of the four homologues of the *Arabidopsis VEGETATIVE STORAGE PROTEIN 2* (*SlVSP2*) genes, *SlVSP2a*, *SlVSP2b* and *SlVSP2c* (Fig. 4k–n), as well as the tomato *PLANT DEFENSIN 1.2* (*SlPDF1.2*), were significantly reduced in *pad* plants (Fig. 4o). Taken together, these results show that the loss of *SlSSI2* gene function leads to alterations in JA content and JA-responsive signalling cascades.

Disruption of *PAD/SlSSI2* increases SA accumulation and SA-dependent responses

Reduced *SSI2* gene function is associated with the accumulation of SA in various plant species, including *Arabidopsis* (Kachroo *et al.* 2001), soybean (Kachroo *et al.* 2008), rice (Jiang *et al.* 2009), and cotton (Mo *et al.* 2021). Hence, SA content levels were measured to examine whether the loss of *PAD/SlSSI2* gene function also induced a similar response. Determination of the endogenous SA content revealed a significantly higher accumulation of SA in *pad* mutants compared to WT plants (Fig. 5a). The *pad* leaves accumulated a mean SA content of 49.45 ± 24.31 ng·g^{-1} FW *versus* 270.25 ± 98.32 ng·g^{-1} FW in the WT. Additionally, the expression levels

of SA biosynthesis and signalling related genes were determined by qRT-PCR in WT and *pad* plants. Despite the SA content increase observed in *pad* plants, they showed a significant decrease in expression levels of the tomato homologues of the *Arabidopsis ISOCHORISMATE SYNTHASE 1* (*SlICS1*) and *PHENYLALANINE AMMONIA LYASE 1* (*SlPAL1*) (Fig. 5b, c), two key SA biosynthetic genes in the isochorismate (ICS) and phenylalanine ammonia-lyase (PAL) pathways, respectively (Lefevere *et al.* 2020). Moreover, the expression of one of the two homologues of the *Arabidopsis ENHANCED DISEASE SUSCEPTIBILITY 5* (*SlEDS5b*), a transporter protein of the SA biosynthetic precursor (ICS) from the chloroplast to the cytoplasm (Serrano *et al.* 2013), was significantly downregulated in *pad*, whereas no significant differences were observed for *SlEDS5a* (Fig. 5d, e). In contrast, expression levels of the homologues of *ENHANCED DISEASE SUSCEPTIBILITY 1* (*SlEDS1*) and *PHYTOALEXIN DEFICIENT 4* (*SlPAD4*), which play a crucial role in promoting SA accumulation in *Arabidopsis* (Cui *et al.* 2017), were upregulated in *pad* leaves (Fig. 5f, g). Furthermore, the transcript levels of 5 of the 7 evaluated homologues of the Arabidopsis SA-responsive gene *PATHOGENESIS-RELATED GENE 1* (*SlPR1*), *SlPR1a*, *SlPR1b*, *SlPR1c*, *SlPR1f* and *SlPR1g*, were significantly higher in *pad* plants (Fig. 5h–l). Expression of *SlPR1d* and *SlPR1e* genes was not detected in either WT or *pad* plants. Collectively, these results indicate that *pad* mutation leads to SA accumulation and activates the SA-mediated defence signalling pathway.

DISCUSSION

The identification and functional characterization of *pad* allowed us to isolate the *PAD/SlSSI2* gene coding for a plastid localized isoform of SACPD, which could be considered as a putative orthologue of the *Arabidopsis* SSI2. Our work reports for the first time the function of *SSI2* in tomato and reveals that its disruption leads to severe alterations in plant growth

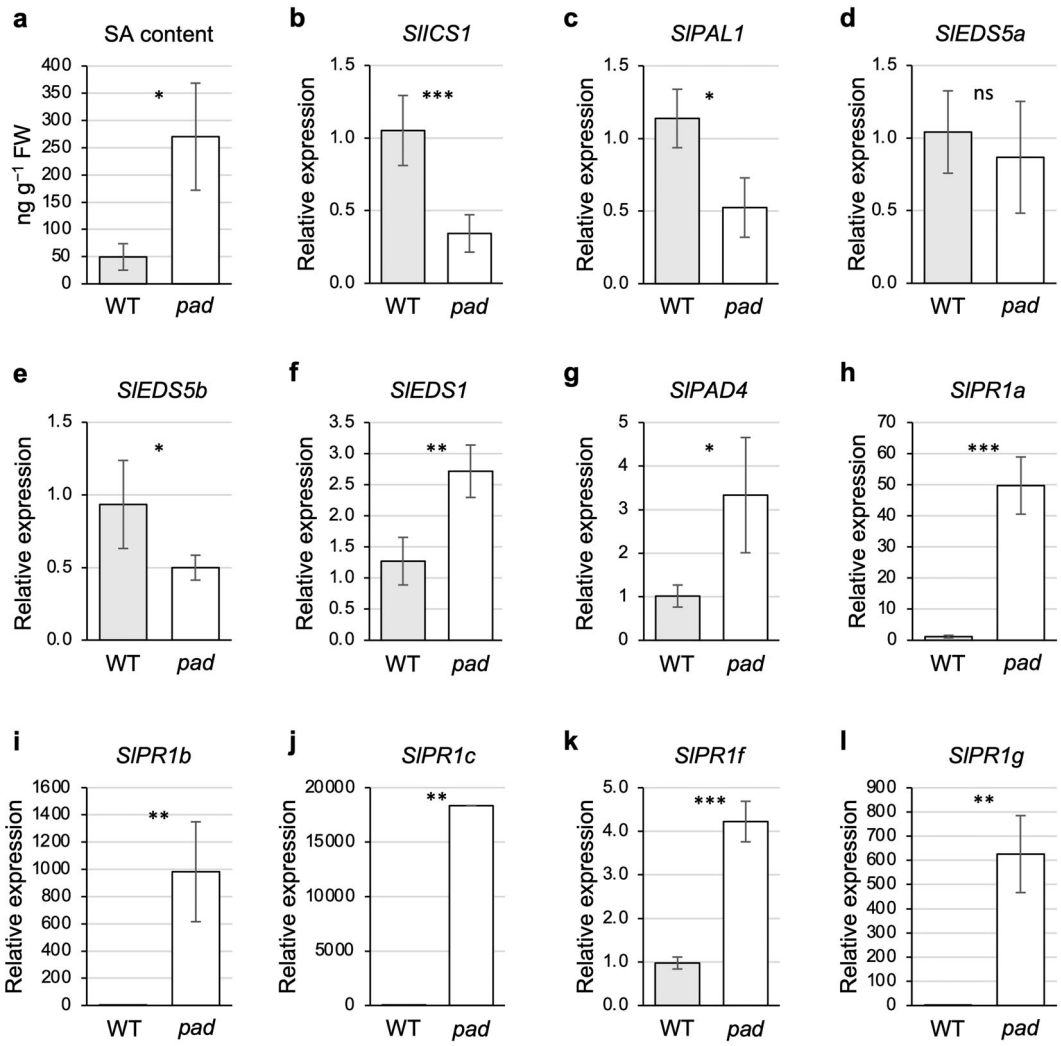

Fig. 5. Salicylic acid (SA) content and relative expression levels of SA-related genes in wild-type (WT) and *pad* mutant plants. (a) Quantification of SA in leaves of WT and *pad* plants. (b–l) Relative expression by qRT-PCR of SA biosynthetic genes *SlICS1* (b), *SlPAL1* (c), *SlEDS5a* (d) and *SlEDS5b* (e), SA accumulation genes *SlEDS1* (f) and *SlPAD4* (g), and SA signalling pathway genes *SlPR1a* (h), *SlPR1b* (i), *SlPR1c* (j), *SlPR1f* (k) and *SlPR1g* (l) in leaf tissues of WT and *pad* plants. Significant differences detected using Student's *t*-test are represented by asterisks: *$P < 0.01$; **$P < 0.001$; ***$P < 0.0001$; ns, no statistically significant differences.

and development, giving rise to pale and dwarf plants, a phenotype similar to those observed in other plant species after losing the function of *SSI2*, such as *Arabidopsis* (Kachroo *et al.* 2001), soybean (Kachroo *et al.* 2008), rice (Jiang *et al.* 2009), and cotton (Mo *et al.* 2021). Such developmental alterations are associated with the accumulation of 18:0 fatty acid, as *SSI2* regulates levels of unsaturated fatty acids in cells mediating the conversion of 18:0-ACP to 18:1-ACP. Since 18:1-ACP is the main substrate for the formation of mono- and digalactosyl diacylglycerol membrane glycerolipids, mutations in *SSI2* impair membrane integrity, which further affect chlorophyll biosynthesis and photosynthesis efficiency, giving rise to progressive chlorosis and the occurrence of necrotic lesions (Kobayashi *et al.* 2016; He *et al.* 2020) comparable to those observed in *pad* mutant plants. Accordingly, the pale colour and the subsequent lethality of the tomato *pad* mutant plants are mainly caused by their deficient production of 18:1 fatty acid, thus revealing that *PAD/SlSSI2* gene function is crucial for correct tomato growth and development. In agreement with its essential function, *PAD/SlSSI2* showed a ubiquitous expression profile during tomato plant development, although the levels of expression were variable among tissues, finding its highest expression in leaves, as well as flowers at anthesis day and fruits at red stage. Consequently, the observed expression pattern suggests that *PAD/SlSSI2* is not only involved in vegetative plant growth but also in reproductive development. In support of this hypothesis, it has been demonstrated that the reduction in 18:1 fatty acid content resulting from the loss of function of the *Arabidopsis SSI2* gene leads to nitric oxide accumulation (Mandal *et al.* 2012). Nitric oxide acts as a signalling molecule in several physiological processes, including flowering, where elevated endogenous nitric oxide levels have been shown to repress floral transition (He *et al.* 2004; Besson-Bard *et al.* 2008; Wilson *et al.* 2008). Although further studies are needed to support the involvement of nitric oxide in tomato flowering, it is plausible to hypothesize that mutations in the tomato *PAD/SlSSI2* gene might cause changes in nitric oxide homeostasis, thereby explaining why neither *pad* nor CRISPR/Cas9 plants were able to flower.

As SACPD is involved in unsaturated fatty acid biosynthesis, mutations in *PAD/SlSSI2* gave rise to reduced levels of the JA precursor 18:3 fatty acid. Similar results were found in plants with loss of function of *SSI2* homologues in rice (Jiang *et al.* 2009) and cotton (Mo *et al.* 2021), which had decreased 18:3 levels. In contrast, *Arabidopsis ssi2* mutant plants, although also contained greatly reduced 18:1 levels, showed 18:3 content comparable with WT plants (Kachroo *et al.* 2001). Similarly, *GmSACPD*-silenced plants in soybean had decreased 18:1 levels, but no alterations in 18:3 content (Kachroo *et al.* 2008). Although the SACPD family occurs throughout the plant kingdom, these results suggest a functional diversification of SACPD enzymes in different plant species promoting divergent catalytic capabilities and synthesis of novel fatty acids and derivatives, which could explain the differences in the chemical properties of membranes and storage lipids found in crop species. In agreement with this hypothesis, our phylogenetic analysis revealed divergences in the composition of the SACPD subfamily in *Arabidopsis* and tomato, with seven and nine members, respectively (Figure S1). Thus, in *Arabidopsis* the stearoyl-acyl carrier protein 9-desaturase 1 subfamily is composed of five genes, whereas the tomato genome does not encode any member of this subfamily. Conversely, the stearoyl-acyl carrier protein 9-desaturase 6 subfamily in *Arabidopsis* has a single member, but in tomato is constituted by six genes. With regard to the stearoyl-acyl carrier protein 9-desaturase 7 subfamily, where *SSI2* homologues are located, it consists of one and three members for *Arabidopsis* and tomato, respectively. Despite the existence of several tomato genes in this subfamily, our results indicate that the loss of function of *PAD/SlSSI2* is enough to produce dramatic phenotypic defects in tomato. This observation suggests that SACPD genes may not perform redundant functions, although it is also possible that the enzymes encoded by these genes can desaturate 18:0-ACP but with decreased activity, as is the case of *Arabidopsis* where SACPD isozymes have greatly reduced specific activity as compared to SSI2 (Kachroo *et al.* 2007). Further studies into the potential functions of tomato SACPD genes will help to decipher their role in mediating unsaturated fatty acid production, as well as their implications in plant growth and development.

Jasmonic acid biosynthesis is initiated by the release of 18:3 fatty acid through hydrolysis of the chloroplast membranes by phospholipases (Wasternack & Song 2017). Hence, the reduced levels of 18:3 in *pad* mutants seem to be responsible for the decrease in JA content. The basic-helix–loop–helix transcription factor MYC2 has been reported as the master transcriptional regulator of JA-mediated signalling (Kazan & Manners 2013). The MYC2 function depends on its physical interaction with the MED25 subunit of the Mediator transcriptional coactivator complex. At a lower level of JA, the MYC2 function is suppressed by JAZ proteins, which block the binding of MYC2 to the co-activator MED25 (Zhang *et al.* 2015; An *et al.* 2017). Remarkably, despite the low JA content observed in tomato *pad* mutants, *SlMYC2* and *SlMED25* were upregulated, whereas *SlJAZ1* was found to be downregulated, suggesting the existence of a parallel pathway that activates the expression of *SlMYC2* independently of JA levels. The formation of the MYC2-MED25 complex is also impaired by MTB proteins, which compete with MYC2 to form a negative feedback circuit to terminate JA-responsive gene expression (Liu *et al.* 2019). Our expression data revealed the upregulation of *MTB2* and *MTB3* in *pad* plants, which suggests that even though *SlMYC2* is overexpressed, it is not sufficient to activate JA-responsive signalling cascades, likely due to its interaction with MTB proteins. In agreement with this hypothesis, JA responsive genes such as *SlVSP2a*, *SlVSP2b*, *SlVSP2c* and *SlPDF1.2* were inhibited in *pad* plants indicating that the loss of *PAD/SlSSI2* function results in a deregulation of the genetic network controlling the JA signalling pathway.

Salycylic acid is synthesized *via* two possible pathways involving ICS or PAL enzymes. The importance of the two pathways for SA biosynthesis differs between plant species. Thus, the ICS is the main pathway for SA accumulation in *Arabidopsis*, whereas the PAL pathway is most important in rice. In other species, such as soybean, both pathways contribute equally to increase SA content (Shine *et al.* 2016). Our findings showed that the loss of *PAD/SlSSI2* function alters the expression of *SlICS1* and *SlPAL1*, two key SA biosynthetic genes in ICS and PAL pathways. These results suggest that both ICS- and PAL-mediated pathways may contribute similarly to SA biosynthesis in tomato, although further experiments are required to confirm this hypothesis. Despite the high SA levels found in *pad* mutants, they showed reduced

expression of *SlICS1* and *SlPAL1*, which leads us to speculate that the continuous accumulation of SA in *pad* plants may finally result in the inhibition of SA biosynthetic genes. The antagonistic crosstalk between SA and JA signalling pathways is particularly well characterized (Thaler *et al.* 2012) and was first reported in tomato, where SA application blocked both JA production and JA-mediated transcription of protease inhibitors involved in defence against insects (Pena-Cortés *et al.* 1993; Doares *et al.* 1995). In this regard, it has been reported that SA accumulation positively regulates the expression of *EDS1* and *PAD4*, which in turn form a protein complex to inhibit molecular component of JA-mediated signalling such as *MYC2* (Cui *et al.* 2018). In *pad* plants, *SlEDS1*, *SlPAD4* and *SlMYC2* were upregulated, revealing that high SA content boosts *SlEDS1* and *SlPAD4* transcript levels although not enough to repress *SlMYC2*, which suggests that *SlMYC2* expression is also induced by other SA-independent mechanisms. Taken together, our results are consistent with the existence of this cross-communication between SA and JA pathways, as *pad* mutants accumulated SA to high levels and had diminished JA content, which resulted in a constitutively activated SA-mediated defence signalling response and an inhibited JA-responsive signalling pathway.

In summary, our findings revealed that both the original T-DNA insertional *pad* mutant and CRISPR/Cas9 lines bear putative knockout alleles of *PAD/SlSSI2*, which lead to a lethal phenotype, revealing the crucial function of *PAD/SlSSI2* for correct tomato growth and development. Thus, this study lays the foundation for further research on fatty acid desaturases in tomato, which will provide a better insight into the metabolic effect of the polyunsaturated fatty acid profile on plant performance and fitness in this crop species.

ACKNOWLEDGEMENTS

This work was supported by research grants PID2019-110833RB-C31 and PID2019-110833RB-C32 funded by the Spanish Ministry of Science and Innovation (MCIN/AEI/10.13039/501100011033), and the Research and Innovation Programme of the European Union Horizon 2020 (BRESOV Project, ID 774244). The authors thank Campus de Excelencia Internacional Agroalimentario (CeiA3) for providing research facilities.

AUTHOR CONTRIBUTIONS

F. J. Yuste-Lisbona, **V. Moreno**, **T. Angosto** and **R. Lozano** conceived and designed research. **A. S. Quevedo-Colmena**, **A. Ortiz-Atienza**, **M. Jáquez-Gutiérrez**, and **M. Quinet** performed research. **M. Quinet**, **A. Atarés**, **F. J. Yuste-Lisbona**, **V. Moreno**, **T. Angosto** and **R. Lozano** contributed new reagents or analytical tools. **A. S. Quevedo-Colmena**, **F. J. Yuste-Lisbona**, **T. Angosto** and **R. Lozano** analysed data. **A. S. Quevedo-Colmena**, **F. J. Yuste-Lisbona**, **T. Angosto** and **R. Lozano** wrote the manuscript. All authors read and approved the manuscript.

CONFLICT OF INTEREST

The authors declare that they have no conflict of interest.

DATA AVAILABILITY STATEMENT

All data generated or analysed during this study are included in this published article and its supplementary information files.

SUPPORTING INFORMATION

Additional supporting information may be found online in the Supporting Information section at the end of the article.

Figure S1. Phylogenic tree of tomato and *Arabidopsis* stearoyl-acyl carrier protein desaturase family.

Figure S2. Nucleotide sequence alignment of the wild-type (WT) *SlSSI2* sequence with the sequence of the CR-*Slssi2* edited alleles schematized in Fig. 3.

Figure S3. Amino acid sequence alignment of the wild-type (WT) SlSSI2 protein with the predicted proteins generated from the CR-*Slssi2* edited alleles obtained in this work.

Table S1. Primer sequences used for anchor-PCR, *SlSSI2* genotyping and CRISPR/Cas9 assays.

Table S2. Primer sequences used for qRT-PCR expression analysis.

Table S3. Fatty acid composition of total leaf lipids from wild-type, *pad* and CR-*Slssi2* plants.

REFERENCES

An C., Li L., Zhai Q., You Y., Deng L., Wu F., Chen R., Jiang H., Wang H., Chen Q., Li C. (2017) Mediator subunit MED25 links the jasmonate receptor to transcriptionally active chromatin. *Proceedings of the National Academy of Sciences of the United States of America*, **114**, E8930–E8939.

Arnon D.I. (1949) Copper enzymes in isolated chloroplasts. Polyphenoloxidase in *Beta vulgaris*. *Plant Physiology*, **24**, 1–15.

Atarés A., Moyano E., Morales B., Schleicher P., García-Abellán J.O., Antón T., García-Sogo B., Perez-Martin F., Lozano R., Flores F.B., Moreno V., Bolarin M.C., Pineda B. (2011) An insertional mutagenesis programme with an enhancer trap for the identification and tagging of genes involved in abiotic stress tolerance in the tomato wild-related species *Solanum pennellii*. *Plant Cell Reports*, **30**, 1865–1879.

Besson-Bard A., Pugin A., Wendehenne D. (2008) New insights into nitric oxide signaling in plants. *Annual Review of Plant Biology*, **59**, 21–39.

Chandra-Shekara A.C., Venugopal S.C., Barman S.R., Kachroo A., Kachroo P. (2007) Plastidial fatty acid levels regulate resistance gene-dependent defense signaling in Arabidopsis. *Proceedings of the National Academy of Sciences of the United States of America*, **104**, 7277–7282.

Chen P.Y., Wang C.K., Soong S.C., To K.Y. (2003) Complete sequence of the binary vector pBI121 and its application in cloning T-DNA insertion from transgenic plants. *Molecular Breeding*, **11**, 287–293.

Cui H., Gobbato E., Kracher B., Qiu J., Bautor J., Parker J.E. (2017) A core function of EDS1 with PAD4 is to protect the salicylic acid defense sector in Arabidopsis immunity. *New Phytologist*, **213**, 1802–1817.

Cui H., Qiu J., Zhou Y., Bhandari D.D., Zhao C., Bautor J., Parker J.E. (2018) Antagonism of transcription factor MYC2 by EDS1/PAD4 complexes bolsters salicylic acid defense in Arabidopsis effector-triggered immunity. *Molecular Plant*, **11**, 1053–1066.

Dahmer M.L., Fleming P.D., Collins G.B., Hildebrand D.F. (1989) A rapid screening technique for determining the lipid composition of soybean seeds. *Journal of the American Oil Chemists' Society*, **66**, 543–548.

Doares S.H., Narvaez-Vasquez J., Conconi A., Ryan C.A. (1995) Salicylic acid inhibits synthesis of proteinase inhibitors in tomato leaves induced by systemin and jasmonic acid. *Plant Physiology*, **108**, 1741–1746.

Ellul P., Garcia-Sogo B., Pineda B., Ríos G., Roig L.A., Moreno V. (2003) The ploidy level of transgenic plants in *Agrobacterium*-mediated transformation of tomato cotyledons (*Lycopersicon esculentum* Mill.) is genotype and procedure dependent. *Theoretical and Applied Genetics*, **106**, 231–238.

Gao Q.M., Venugopal S., Navarre D., Kachroo A. (2011) Low oleic acid-derived repression of jasmonic acid-inducible defense responses requires the WRKY50 and WRKY51 proteins. *Plant Physiology*, **155**, 464–476.

He M., Qin C.X., Wang X., Ding N.Z. (2020) Plant unsaturated fatty acids: biosynthesis and regulation. *Frontiers in Plant Science*, **11**, 390.

He Y., Tang R.H., Hao Y., Stevens R.D., Cook C.W., Ahn S.M., Jing L., Yang Z., Chen L., Guo F., Fiorani F., Jackson R.B., Crawford N.M., Pei Z.M. (2004) Nitric oxide represses the Arabidopsis floral transition. *Science*, **305**, 1968–1971.

Jiang C.J., Shimono M., Maeda S., Inoue H., Mori M., Hasegawa M., Sugano S., Takatsuji H. (2009) Suppression of the rice fatty-acid desaturase gene *OsSSI2* enhances resistance to blast and leaf blight diseases in rice. *Molecular Plant-Microbe Interactions*, **22**, 820–829.

Kachroo A., Fu D.Q., Havens W., Navarre D., Kachroo P., Ghabrial S.A. (2008) An oleic acid-mediated pathway induces constitutive defense signaling and enhanced resistance to multiple pathogens in soybean. *Molecular Plant-Microbe Interactions*, **21**, 564–575.

Kachroo A., Lapchyk L., Fukushige H., Hildebrand D., Klessig D., Kachroo P. (2003) Plastidial fatty acid signaling modulates salicylic acid- and jasmonic acid-mediated defense pathways in the Arabidopsis *ssi2* mutant. *The Plant Cell*, **15**, 2952–2965.

Kachroo A., Shanklin J., Whittle E., Lapchyk L., Hildebrand D., Kachroo P. (2007) The Arabidopsis stearoyl-acyl carrier protein-desaturase family and the contribution of leaf isoforms to oleic acid synthesis. *Plant Molecular Biology*, **63**, 257–271.

Kachroo A., Venugopal S.C., Lapchyk L., Falcone D., Hildebrand D., Kachroo P. (2004) Oleic acid levels regulated by glycerolipid metabolism modulate defense gene expression in Arabidopsis. *Proceedings of the National Academy of Sciences of the United States of America*, **101**, 5152–5157.

Kachroo P., Shanklin J., Shah J., Whittle E.J., Klessig D.F. (2001) A fatty acid desaturase modulates the activation of defense signaling pathways in plants. *Proceedings of the National Academy of Sciences of the United States of America*, **98**, 9448–9453.

Kazan K., Manners J.M. (2013) MYC2: the master in action. *Molecular Plant*, **6**, 686–703.

Kobayashi K., Endo K., Wada H. (2016) Roles of lipids in photosynthesis. *Sub-Cellular Biochemistry*, **86**, 21–49.

Lefevere H., Bauters L., Gheysen G. (2020) Salicylic acid biosynthesis in plants. *Frontiers in Plant Science*, **11**, 338.

Li L., Zhao Y., McCaig B.C., Wingerd B.A., Wang J., Whalon M.E., Pichersky E., Howe G.A. (2004) The tomato homolog of CORONATINE-INSENSITIVE1 is required for the maternal control of seed maturation, jasmonate-signaled defense responses, and glandular trichome development. *The Plant Cell*, **16**, 126–143.

Lichtenthaler H.K., Wellburn A.R. (1983) Determinations of total carotenoids and chlorophylls *a* and *b* of leaf extracts in different solvents. *Biochemical Society Transactions*, **11**, 591–592.

Liu Y., Du M., Deng L., Shen J., Fang M., Chen Q., Lu Y., Wang Q., Li C., Zhai Q. (2019) MYC2 regulates the termination of jasmonate signaling via an autoregulatory negative feedback loop. *The Plant Cell*, **31**, 106–127.

Major I.T., Yoshida Y., Campos M.L., Kapali G., Xin X.F., Sugimoto K., de Oliveira Ferreira D., He S.Y., Howe G.A. (2017) Regulation of growth–defense balance by the JASMONATE ZIM-DOMAIN (JAZ)-MYC transcriptional module. *New Phytologist*, **215**, 1533–1547.

Mandal M.K., Chandra-Shekara A.C., Jeong R.D., Yu K., Zhu S., Chanda B., Navarre D., Kachroo A., Kachroo P. (2012) Oleic acid-dependent modulation of NITRIC OXIDE ASSOCIATED1 protein levels regulates nitric oxide-mediated defense signaling in Arabidopsis. *The Plant Cell*, **24**, 1654–1674.

Mo S., Zhang Y., Wang X., Yang J., Sun Z., Zhang D., Chen B., Wang G., Ke H., Liu Z., Meng C., Li Z., Wu L., Zhang G., Duan H., Ma Z. (2021) Cotton GhSSI2 isoforms from the stearoyl acyl carrier protein fatty acid desaturase family regulate *Verticillium* wilt resistance. *Molecular Plant Pathology*, **22**, 1041–1056.

Ohlrogge J., Browse J. (1995) Lipid biosynthesis. *The Plant Cell*, **7**, 957–970.

Oliveros J.C., Franch M., Tabas-Madrid D., San-León D., Montoliu L., Cubas P., Pazos F. (2016) Breaking-Cas-interactive design of guide RNAs for CRISPR-Cas experiments for ENSEMBL genomes. *Nucleic Acids Research*, **44**, W267–W271.

Pena-Cortés H., Albrecht T., Prat S., Weiler E.W., Willmitzer L. (1993) Aspirin prevents wound-induced gene-expression in tomato leaves by blocking jasmonic acid biosynthesis. *Planta*, **191**, 123–128.

Pérez-Martín F., Yuste-Lisbona F.J., Pineda B., Angarita-Díaz M.P., García-Sogo B., Antón T., Sánchez S., Giménez E., Atarés A., Fernández-Lozano A., Ortíz-Atienza A., García-Alcázar M., Castañeda L., Fonseca R., Capel C., Goergen G., Sánchez J., Quispe J.L., Capel J., Angosto T., Moreno V., Lozano R. (2017) A collection of enhancer trap insertional mutants for functional genomics in tomato. *Plant Biotechnology Journal*, **15**, 1439–1452.

Pérez-Martín F., Yuste-Lisbona F.J., Pineda B., García-Sogo B., Olmo I.D., de Dios Alché J., Egea I., Flores F.B., Piñeiro M., Jarillo J.A., Angosto T., Capel J., Moreno V., Lozano R. (2018) Developmental role of the tomato Mediator complex subunit MED18 in pollen ontogeny. *The Plant Journal*, **96**, 300–315.

Seo M., Jikumaru Y., Kamiya Y. (2011) Profiling of hormones and related metabolites in seed dormancy and germination studies. *Methods in Molecular Biology*, **773**, 99–111.

Serrano M., Wang B., Aryal B., Garcion C., Abou-Mansour E., Heck S., Geisler M., Mauch F., Nawrath C., Métraux J.P. (2013) Export of salicylic acid from the chloroplast requires the multidrug and toxin extrusion-like transporter EDS5. *Plant Physiology*, **162**, 1815–1821.

Shah J., Kachroo P., Nandi A., Klessig D.F. (2001) A recessive mutation in the Arabidopsis *SSI2* gene confers SA- and NPR1-independent expression of *PR* genes and resistance against bacterial and oomycete pathogens. *The Plant Journal*, **25**, 563–574.

Shine M.B., Yang J.W., El-Habbak M., Nagyabhyru P., Fu D.Q., Navarre D., Ghabrial S., Kachroo P., Kachroo A. (2016) Cooperative functioning between phenylalanine ammonia lyase and isochorismate synthase activities contributes to salicylic acid biosynthesis in soybean. *New Phytologist*, **212**, 627–636.

Somerville C., Browse J., Jaworski J.G., Ohlrogge J.B. (2000) Lipids. In: Buchanan B., Gruissem W., Jones R. (Eds), *Biochemistry and molecular biology of plants*. American Society of Plant Physiologists, Rockville, MD, USA, pp 456–527.

Suza W.P., Rowe M.L., Hamberg M., Staswick P.E. (2010) A tomato enzyme synthesizes (+)-7-iso-jasmonoyl-L-isoleucine in wounded leaves. *Planta*, **231**, 717–728.

Thaler J.S., Humphrey P.T., Whiteman N.K. (2012) Evolution of jasmonate and salicylate signal crosstalk. *Trends in Plant Science*, **17**, 260–270.

Tomato Genome Consortium (2012) The tomato genome sequence provides insights into fleshy fruit evolution. *Nature*, **485**, 635–641.

van Meer G., Voelker D., Feigenson G. (2008) Membrane lipids: where they are and how they behave. *Nature Reviews Molecular Cell Biology*, **9**, 112–124.

Vazquez-Vilar M., Bernabé-Orts J.M., Fernandez-Del-Carmen A., Ziarsolo P., Blanca J., Granell A., Orzaez D. (2016) A modular toolbox for gRNA-Cas9 genome engineering in plants based on the GoldenBraid standard. *Plant Methods*, **12**, 10.

Venugopal S.C., Jeong R.D., Mandal M.K., Zhu S., Chandra-Shekara A.C., Xia Y., Hersh M., Stromberg A.J., Navarre D., Kachroo A., Kachroo P. (2009) Enhanced disease susceptibility 1 and salicylic acid act redundantly to regulate resistance gene-mediated signaling. *PLoS Genetics*, **5**, e1000545.

Wasternack C., Song S. (2017) Jasmonates: biosynthesis, metabolism, and signaling by proteins activating and repressing transcription. *Journal of Experimental Botany*, **68**, 1303–1132.

Webb M.S., Green B.R. (1991) Biochemical and biophysical properties of thylakoid acyl lipids. *Biochimica et Biophysica Acta*, **1060**, 133–158.

Wilson I.D., Neil S.J., Hancock J.T. (2008) Nitric oxide synthesis and signalling in plants. *Plant, Cell & Environment*, **31**, 622–631.

Winer J., Jung C.K., Shackel I., Williams P.M. (1999) Development and validation of real-time quantitative reverse transcriptase-polymerase chain reaction for monitoring gene expression in cardiac myocytes *in vitro*. *Analytical Biochemistry*, **270**, 41–49.

Xia Y., Gao Q.M., Yu K., Lapchyk L., Navarre D., Hildebrand D., Kachroo A., Kachroo P. (2009) An intact cuticle in distal tissues is essential for the induction of systemic acquired resistance in plants. *Cell Host & Microbe*, **5**, 151–165.

Yan L., Zhai Q., Wei J., Li S., Wang B., Huang T., Du M., Sun J., Kang L., Li C.B., Li C. (2013) Role of tomato lipoxygenase D in wound-induced jasmonate biosynthesis and plant immunity to insect herbivores. *PLoS Genetics*, **9**, e1003964.

Zhang F., Yao J., Ke J., Zhang L., Lam V.Q., Xin X.F., Zhou X.E., Chen J., Brunzelle J., Griffin P.R., Zhou M., Xu H.E., Melcher K., He S.Y. (2015) Structural basis of JAZ repression of MYC transcription factors in jasmonate signalling. *Nature*, **525**, 269–273.